Biophysical Chemistry 182 (2013) 86–93

Contents lists available at ScienceDirect

Biophysical Chemistry

journal homepage: http://www.elsevier.com/locate/biophyschem

A micro-environmental study of the Zn^{+2}–$A\beta_{1-16}$ structural properties

A. Maiorana [a], T. Marino [b], V. Minicozzi [c,*], S. Morante [c], N. Russo [b]

[a] Università Cattolica del Sacro Cuore, Largo Agostino Gemelli, 8, 00168 Rome, Italy
[b] Dipartimento di Chimica — Università della Calabria, Cubo 12C Via P. Bucci, 87036 Arcavacata di Rende, CS, Italy
[c] Dipartimento di Fisica Università di Roma "Tor Vergata" & INFN, Sezione di Roma "Tor Vergata", Via della Ricerca Scientifica, 1, 00133 Rome, Italy

HIGHLIGHTS

- We performed classical MD of Ab(1–16) in gas phase and in water.
- We used three different classical force fields.
- We performed QM/MM optimization of the MD simulated systems.
- We computed partial charges of QM/MM optimized systems.
- FF3 partial charges match those coming from QM computation and Zn geometry fits the experimentally known metal coordination

GRAPHICAL ABSTRACT

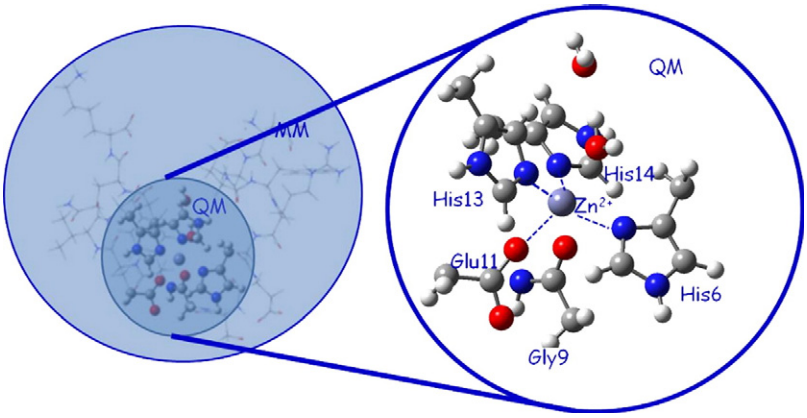

ARTICLE INFO

Article history:
Received 15 April 2013
Received in revised form 14 June 2013
Accepted 7 July 2013
Available online 23 July 2013

Keywords:
Metal
Molecular dynamics
QM/MM
Abeta peptide
Alzheimer

ABSTRACT

Relying on a combination of classical molecular dynamics and hybrid QM/MM computational methods, we study the influence of the nature of the local physico-chemical environment on the structural features of β-amyloid peptides complexed with Zn^{+2} ions. The analysis is carried out by comparing among themselves different Zn^{+2}-ligand force fields and studying their influence on metal coordination and long-range peptide folding. The system in the non-physiological so-called "gas phase" (no solvent) was also simulated with the purpose of identifying to what extent, if at all, the solvent can affect the Zn coordination mode, besides its long-range structural properties. There are two main results of this investigation. The first is that the Zn^{+2} coordination mode in classical molecular dynamics simulations markedly depends on the partial charge attributed to the ion and the atoms surrounding it. Comparing with experiments, it is possible to identify the most appropriate Zn^{+2} force field for the Zn^{+2}–$A\beta_{1-16}$ complex in study. Secondly, although the presence of water naturally influences the peptide folding propensity, it does not affect the structure of the Zn^{+2} inner coordination shell. A useful way to validate classical results and in particular those referring to the structural differences visible when different force fields are employed, was to use a hybrid QM/MM optimization step. When the classical system configurations are submitted to such a quantum minimization step, the geometries of the resulting Zn^{+2} site turn out to be all very similar and structurally in good agreement with what is experimentally known.

1. Introduction

A key feature in the development of the Alzheimer disease (AD) is the formation of plaques made by β-amyloid peptide (Aβ-peptide)

* Corresponding author. Tel.: +39 06 72594554; fax: +39 06 2023507.
E-mail address: minicozzi@roma2.infn.it (V. Minicozzi).

0301-4622/$ – see front matter © 2013 Elsevier B.V. All rights reserved.
http://dx.doi.org/10.1016/j.bpc.2013.07.002

fibrils [1–3]. At the basis of fibril formation there is a conformational change of the Aβ-peptide that leads to the formation of extended β-sheet like structures, capable of aggregating other peptides in long β-sheets with inter-molecular binding.

Metal ions like Cu, Zn and Fe, have been shown to be involved in some key steps of the Aβ aggregation cascade [4,5], although their precise role is not yet fully understood. Copper and zinc are able to bind Aβ directly and modulate aggregation in vitro. Evidence that this can also happen in vivo has come from the finding that Zn and Cu were detected at elevated concentrations in AD patient amyloid plaques [6,7]. Subsequent spectroscopic studies on amyloid plaques suggested that these metals are bound to Aβ [8–13].

In the years quite a number of extensive experimental and theoretical studies have been carried out on metal–Aβ–peptide complexes and a lot of structural information is nowadays available. For instance, it is known that the metal ion binding site is located within the first 16 amino acids of the peptide [11]. Furthermore there is a general consensus on the fact that the Cu^{+2}–Aβ–peptide binding mode is of intramolecular nature [10–12,14–17], while the Zn^{+2} binding is more flexible, and interestingly can even give rise to structures where two peptides are bridged by a single Zn^{+2} ion [10,11,18,19]. Despite all these remarkable experimental efforts, many important details of the atomic arrangement of the Aβ-peptide around the metal are still unknown.

In particular it is not clear where the difference between the Cu^{+2} and Zn^{+2} binding modes [11] comes from. It would certainly be of great interest to be able to elucidate the origin of this difference as it may hint at a different role played by the two metals in the crucial first steps of the fibril aggregation process. Actually there are indications that Cu^{+2} tends to prevent and Zn^{+2} to favor aggregation [11]. At the moment there is not either a clear answer to the key question of what is the correlation (if there is one) between the nature of the metal coordination mode and the peptide propensity to form fibrils.

In this context besides experiments, theoretical investigations based on computer simulations can be of help as they may allow identifying what are the local physico-chemical features that determine the metal coordination mode. This knowledge may hopefully bring some clarification on the apparent different impact of Cu^{+2} and Zn^{+2} ions in the Aβ aggregation processes.

Having in mind this general goal, both Cu^{+2}– and Zn^{+2}–Aβ–peptide complexes have been extensively studied by a number of research groups using *classical* as well as ab initio (quantum-mechanical, QM) simulations [20–30].

One of the major problems with classical molecular dynamics (MD) simulations is the determination and the choice of the partial charges to be attributed to the atoms of the system. Especially delicate is this choice when metal ions are present, because of the need of avoiding giving rise to unphysical Coulomb fields. Force fields of many popular MD codes attribute to metal ions a partial charge that corresponds to their ionization state (i.e. +2 for Cu^{+2}, Zn^{+2}). This choice may lead to a dramatically strong Coulomb potential centered at the metal site, which may result in an unrealistic atom arrangement around the metal center [31]. It is clear that ideally only full-fledged QM calculations can provide effective partial charges for possible later MD simulations. However, such a demanding theoretical work may be unnecessary in many cases as a crude knowledge of partial charges or a more phenomenological "trial and error" approach will be enough for the needs of most MD simulations.

In this work we present the results of extensive combined MD and QM/MM simulations of the Zn^{+2}–$Aβ_{1-16}$ complex with and without water solvent. We have limited our study to the $Aβ_{1-16}$ fragment, because, as we said above, it has been established [11,16] that the metal binding site resides within the first 16 amino acids of the peptide, and we have used the coordination geometry determined in refs. [25,26].

The main purpose of the present investigation is to study to what extent the different classical force fields can affect the local structure of the metal binding site and the long-range arrangement (folding) of the peptide. The study was carried out both in the presence and in the absence of explicit water molecules.

We find that, depending on the partial charge attributed to Zn^{+2} and its ligands, different coordination geometries around the metal are obtained, while naturally water affects the long-range arrangement of the peptide.

These results show that what is crucial in determining the Zn^{+2} local atomic arrangement in classical MD simulations is the correct tuning of the distribution of partial charges among the metal and the surrounding atoms, more than the detailed values of the various force field bonding constants.

This conclusion should sound like obvious given the significantly larger strength of electrostatic forces in comparison with van der Waals forces. However, since, at variance with the rest of the force field, the charge distribution strongly depends on the local geometrical atomic arrangement around the metal, in order to check the reliability of classical MD conclusions, or to refine their outcomes, some sort of *first-principle* calculations is necessary.

Given the size of the molecular system in study (about 1.5×10^4 atoms, including water), the hybrid QM/MM approach [32] was employed for this purpose. The use of this method is particularly well suited here, as it is immediately clear which part of the system should be treated quantum-mechanically (QM → metal ion and the nearest atoms surrounding it) and which part can be treated classically (MM → "rest" of the peptide and water solvent). The structure of the metal site resulting at the end of the QM/MM optimization does not appear to depend on the details of MD force field that was employed to generate the classical simulations. The geometric configuration identified in this way is well compatible with other theoretical studies (see refs. [25,26]) and with experiments (see ref. [33]).

2. Methods

In order to study to what extent the specific features of the Zn^{+2} force field and the presence of the water solvent affect the local coordination geometry of the metal ion and/or the folding property of the peptide at large, we performed extensive classical MD simulations of the Zn^{+2}–$Aβ_{1-16}$ peptide complex in different physico-chemical situations, successively followed by QM/MM optimization steps.

In this section we describe the salient features of the simulation strategy we have followed and give details of the procedure we developed to cope with some of the well-known difficulties of classical MD and hybrid QM/MM simulations and with the unavoidable limitations of computer resources (Table 1).

2.1. Classical MD

In the absence of a commonly accepted Zn^{+2} force field, it is crucial to monitor the possible impact of modifying its parameters and bonding constraints on the resulting geometrical structure of the metal site. To this end we have performed classical MD simulations of the Zn^{+2}–$Aβ_{1-16}$ peptide complex with the help of the open source GROMACS code [34], trying three kinds of Zn^{+2} force fields called *FF1*, *FF2* and *FF3*, respectively, in the following. To comply with the atomic structure of the Zn^{+2} coordination sphere (see the results of ref. [25,26]), in all the force fields we have used, specific bonding interactions between Zn^{+2} and the four His6, His13, His14 and Glu11 residues have been introduced. *FF1* is the standard CHARMM27 force field complemented with the missing bond and angle parameters of Zn^{+2} and its ligands taken from ref. [35]. In *FF2* and *FF3*, bond and angle parameters as

Table 1
$Aβ_{1-43}$ amino acid sequence. Amino- and carboxyl-terminal groups are explicitly displayed.

$Aβ_{1-43}$	H_3N^+-DAEFRHDSGYEVHHQKLVFFAEDVGSNKGAIIGLMVGGVVIAT-COO^-

well as the point charges of Zn^{+2} and its ligands, are taken from ref. [36] and ref. [35], respectively.

In Table 2 we schematically summarize the salient features (concerning bonding constants and partial charge distribution) of the three force fields we have employed, stressing similarities and differences. In Tables T1 and T2 of the supporting information we report the rest of the information on the force fields used for the Zn ion and its ligands.

In the supporting information we also briefly report MD simulations of the $A\beta_{1-16}$ peptide in water and in the gas phase without Zn (using the CHARMM27 force field) that we carried out with the purpose of studying to what extent the presence of Zn^{+2} affects the long-range folding propensity of the peptide. The results of the simulations indicate a little effect of Zn on the long-range peptide structural properties.

Special care has been exerted to identify the "most suited" initial configuration from which to launch our MD simulations that minimizes the well-known bias related to this choice. We decided to pick up the geometry of the PDB structure of ref. [18] (ID: 1ZE9), where three nitrogen and two oxygen atoms lie within the Zn^{+2} coordination sphere, i.e. are at a distance smaller than 2.5 Å.[1] The nitrogen atoms belong to the imidazole ring of His6, His13 and His14. More specifically they are Nδ of His6 and His14, and Nε of His13, while the two oxygen atoms both belong to the Glu11 carboxyl group.

Before starting the actual MD simulations, the PDB configuration was subjected to an energy minimization step (using the standard GROMACS' Conjugate Gradient and Steepest Descent algorithms). The system is then gradually brought to a temperature of 300 K. At this point one continues in the NVT *ensemble* with the temperature kept fixed by means of a Nosè–Hoover thermostat [37]. MD simulations are performed at neutral pH.[2] The dynamics of bound hydrogen atoms is ignored. Solvated systems include 2517 TIP3P water molecules and are contained in a cubic box[3] of side L = 4.272 nm, while systems in vacuum live in box with L = 6.179 nm.[4] Periodic boundary conditions are used throughout. The Particle Mesh Ewald algorithm is employed to deal with Coulomb interactions [38]. A nonbond pair list cutoff of 1.4 nm was used, with the pair list updated every ten steps. For each system in study in the various situations of interest for this paper we have collected 0.75 ns long trajectories. A time step of 1.5 fs was used.

All in all we have performed $3 \times 2 = 6$ independent MD simulations of the Zn^{+2}–$A\beta_{1-16}$ complex corresponding to the three force fields *FF1*, *FF2* and *FF3* we have tried and whether we consider the system in its gas-phase (GP) or in water (W). For short in the following the six simulated models will be labeled with the notation $(S_i)^{GP}$ and $(S_i)^{W}$, i = 1, 2, 3, respectively.

2.2. QM/MM

The QM/MM computational scheme was used to study the quantum-mechanical stability of the system structures obtained from the classical MD simulations described above. The idea of QM/MM is to split the whole system in two layers with the highest-level layer treated quantum-mechanically (QM) and the rest (the lowest-level layer) treated at the molecular mechanical (MM) level. In our case the natural separation of the Zn^{+2}–$A\beta_{1-16}$ complex is to have at the highest level the Zn^{+2} ion and its nearest residues, leaving for the lowest MM level all what is left.

Table 2
The Zn force field parameters of the three force fields used in the paper. The quantities K_b and b_0 are the elastic binding constant and the bond length, respectively.

	Zn point charge	Bond parameters		
FF1	*+2*		K_b (kJ mol^{-1} nm^{-2})	b_0 (nm)
		Zn – N(His)	82804.0	0.205
FF3	*+0.7*	Zn – O(Glu)	110404.0	0.196
FF2	*+0.5*		K_b (kJ mol^{-1} nm^{-2})	b_0 (nm)
		Zn – N(His)	346435.2	0.210
		Zn – O(Glu)	346435.2	0.210

The two-layered hybrid ONIOM [39–41] method, as implemented in the GAUSSIAN-03 code [42], was employed to perform QM/MM simulations. The first layer is treated at the QM level by using the B3LYP hybrid exchange-correlation functional. The QM cluster includes the Zn^{+2} ion and the directly coordinated amino acid residues (His6, His13, His14 and Glu11) plus Gly9 that, although not directly coordinated, is expected to play a significant role owing to its proximity to the metal center. The QM treatment of these amino acids does not include the entire residues but only the imidazole ring and the $C_\beta H_2$ side chain for histidine, carboxylate and the $C_\gamma H_2$ side chain for glutamic acid and the main chain for glycine (see Fig. 1). For H, C, N and O atoms the 6–31 + G(d,p) basis set was used, while for the Zn ion the Stuttgart–Dresden (SDD) valence basis set coupled with their relative pseudopotentials was employed. The second layer that includes the remaining amino acid residues, as well as some moiety of those coordinated to the metal (see above) as well as 2517 water molecules, was treated at the molecular mechanic (MM) level employing the Universal force field (UFF). The parameters of the UFF are estimated using general rules based for each atom only on its nature, hybridization status and connectivity [43].

Like in the case of the MD simulations, also within the QM/MM computational strategy the choice of the particular system configuration that has to be subjected to the quantum-mechanical optimization step is rather delicate. Since the purpose of this part of the work is to verify/check the stability of the classically generated configurations, the problem arises of deciding which ones of the many "pictures" collected along the MD trajectories should undergo the QM/MM step. In order to minimize the bias introduced by this choice, we have devised the following procedure. First of all, we randomly extract from the pool of the available (equilibrated and structurally stable) classical configurations a few of them (about 10) among which we pick up the one that has the lowest potential energy. The atomic coordinates are then moved to bring the system to its mechanical equilibrium by minimizing (via steepest descent) its potential energy. The resulting configuration is the one that is finally exported to ONIOM. This procedure is of course carried out for each of the six MD trajectories that have been generated in correspondence of the six simulated models, $(S_i)^{GP}$ and $(S_i)^{W}$, i = 1, 2, 3.

Finally in order to verify whether the resulting QM/MM geometries are real minima of the potential energy surface, a vibrational analysis was carried out, checking that all the eigenvalues of the relevant Hessian matrices were indeed positive.

3. Results

We now discuss the simulation results we have obtained for the local structure of the peptide around the metal when different force fields are used. We present at the same time a comparison of what we get for the whole system in its gas phase versus what we get in water. We separately illustrate what it is found from classical simulations and the successive QM/MM calculations.

[1] We conventionally define, as it is customary, the metal coordination sphere by assigning to it a radius of 2.5 Å. We say that an atom is coordinated to the metal if it enters the coordination sphere, even if not explicitly bound to the metal.

[2] This means that the protonation state of the peptide was chosen with the N-terminus, arginine and lysine protonated and positively charged while the C-terminus, glutamic and aspartic acid deprotonated and negatively charged. This corresponds to the expected protonation of the free amino acids at neutral pH.

[3] A smaller box has been used in the case of the solvated system, owing to the screening effect of Coulomb potentials offered by the presence of water.

[4] A penta-coordination has been observed in EXAFS experiments on Zn+2–Aβ1–16 complexes in solution with the fifth ligand being a water oxygen [10,11]. In this case, however, four of the ligands are histidines, implying that Zn+2 (which is present at a sub-stoichiometric concentration) is binding pairs of Aβ1–16-peptides.

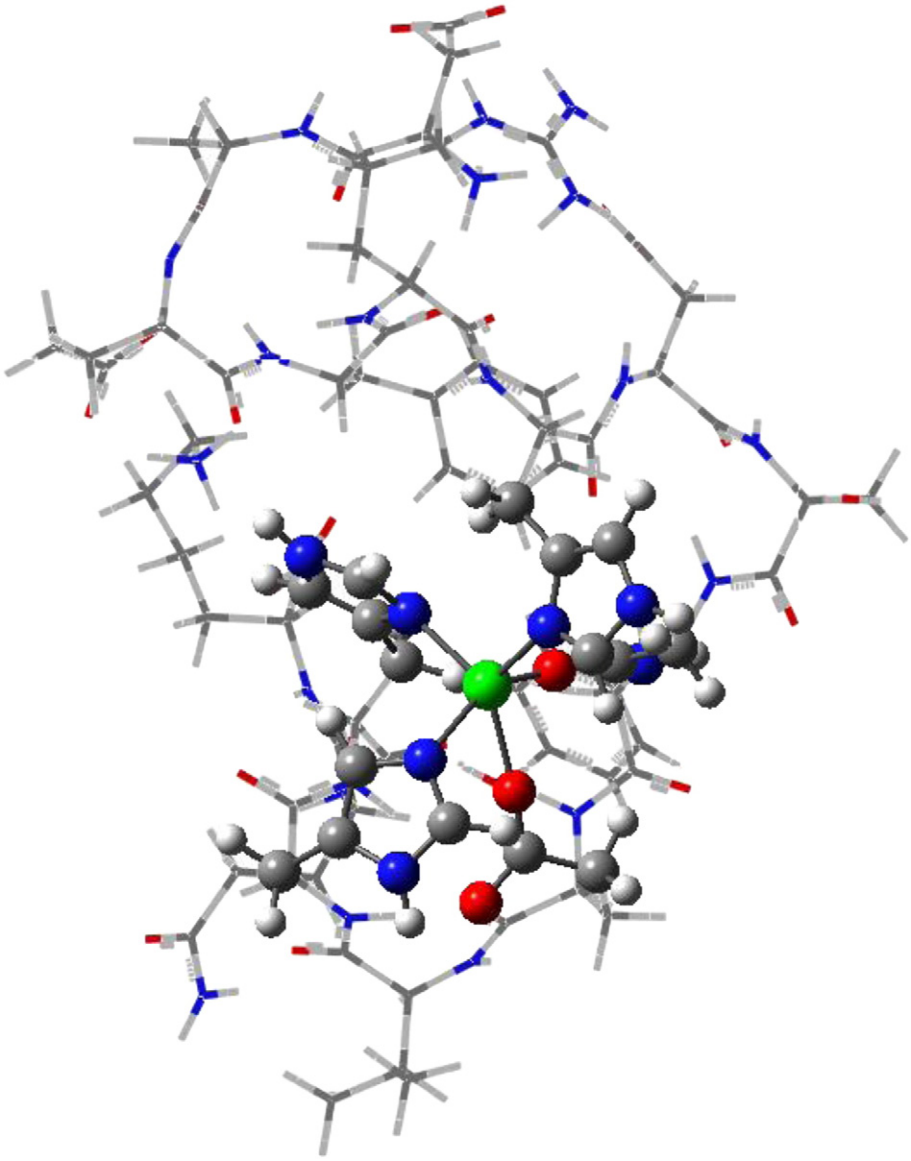

Fig. 1. QM region (ball and stick) and MM region (wireframe).

3.1. Classical MD simulations

We start by illustrating the structural features characterizing the local geometry of the metallic site resulting from the classical MD simulations carried out with the force fields, *FF1*, *FF2* and *FF3* of Table 2, and what is the effect of water. We then pass to discuss how the global folding properties of the peptide are affected by the choice of the force field and the presence of water.

All MD simulations start from the same initial configurations, where Zn^{+2} is coordinated to the four ligands Nδ(His6), Nε(His13), Nδ(His14), and O(Glu11) (see first column of Table 3).

In Table 3 together with the starting configuration (first column), the mean (taken along the MD 300 K simulation) distance from Zn of all the atoms that enter the coordination sphere is reported for every force field both in the gas phase (GS) and in solution (W). The fluctuation width around the mean distance is given in parenthesis.

–*FF1*: From the initial tetra-coordinated metal site structure, interestingly the simulation of the Zn^{+2}–$A\beta_{1-16}$ complex in the gas phase (the $(S_1)^{GP}$ model system) ends up with a penta-coordinated Zn^{+2} geometry with O(Gly9) as a fifth ligand.

When the solvated system, $(S_1)^{W}$, is let to evolve, the structure of the Zn^{+2} site gets further modified as a water molecule enters the metal coordination sphere as a sixth ligand.

Table 3
In the first column we list the atoms lying within the Zn coordination sphere (d ≤ 2.5 Å). In parenthesis we report the amino acids (or water molecule) they belong to. In the second column we give the distance from Zn of the atoms within its coordination sphere at the beginning of classical MD. From columns 3 to 8 the mean distances from the Zn of the atoms entering coordination sphere during the 300 K classical MD simulations in the six model systems we have considered, are listed. Errors are on the last digit and given in parenthesis. They have been computed as the standard deviation along the MD trajectory.

Atom	Distance from Zn (Å)						
	Starting config.	$(S_1)^{GP}$	$(S_1)^{W}$	$(S_2)^{GP}$	$(S_2)^{W}$	$(S_3)^{GP}$	$(S_3)^{W}$
Nδ(His6)	2.10	2.22 (5)	2.28 (6)	2.11 (3)	2.11 (3)	2.08 (6)	2.11 (6)
Oε(Glu11)	2.12	2.15 (5)	2.22 (5)	2.12 (3)	2.13 (3)	2.06 (4)	2.09 (5)
Nε(His13)	2.15	2.14 (5)	2.23 (5)	2.11 (3)	2.11 (3)	2.06 (6)	2.08 (6)
Nδ(His14)	2.29	2.20 (5)	2.31 (5)	2.11 (3)	2.11 (3)	2.08 (5)	2.08 (5)
O(Gly9)		2.14 (9)	2.20 (10)				
$O(H_2O)$			2.19 (9)				

–*FF2*: Along the MD trajectories produced with this force field only little changes occur. In fact, the Zn^{+2} ion remains tetra-coordinated as it is at the beginning of the MD simulation irrespective of the presence of water, i.e. both for the $(S_2)^{GP}$ and $(S_2)^{W}$ systems.
–*FF3*: The situation here is very much like the one we have in the *FF2* case for both $(S_3)^{GP}$ and $(S_3)^{W}$ model systems, with the only small difference that, owing to the fact that bond constants are weaker than in the *FF2* case, now metal–ligand distances fluctuate significantly more than in the previous case, similarly to what happens with *FF1*.

The results reported above indicate that *FF1* is the less realistic of the three force fields as it gives rise to Zn^{+2} local site structures (five ligands in the gas-phase and six ligands in water) that are not the ones emerging from experiments, where indications are that in most proteins Zn^{+2} is tetra-coordinated (see the statistical analysis of ref. [31] and references therein).[5]

An effective way to monitor the overall structural differences possibly emerging from the *FF1*, *FF2* and *FF3* force fields is to measure the relative root mean square distance (RMSD) between pair of configurations. The calculation of RMSD is done by using the standard analysis program provided within the VMD visualization program [44]. It consists of the following steps. First of all, for each trajectory, a cluster analysis of the generated configurations is performed, using the g_cluster GROMACS routine [34]. Clusters of configurations are defined by including in each cluster pairs of configurations whose relative RMSD is smaller than a preassigned threshold that we fixed to 1 Å. It turns out that no matter which system trajectory we take (among $(S_1)^{W}$, $(S_2)^{W}$ or $(S_3)^{W}$) all the configurations belonging to it are very similar so that they all belong to the same cluster. Secondly, for each system we identify within the cluster the most representative among the configurations, as the one that has the smallest average distance to the others. Finally the most representative configuration of each system is used to compute the relative RMSD among $(S_1)^{W}$, $(S_2)^{W}$ or $(S_3)^{W}$, obtaining the following numbers

$$\begin{aligned}
&\mathrm{RMSD}\left[(S_3)^{W}\ \text{vs}\ (S_1)^{W}\right] = 3.5\,\text{Å}\\
&\mathrm{RMSD}\left[(S_2)^{W}\ \text{vs}\ (S_1)^{W}\right] = 2.9\,\text{Å}\\
&\mathrm{RMSD}\left[(S_2)^{W}\ \text{vs}\ (S_3)^{W}\right] = 1.9\,\text{Å}.
\end{aligned}$$

These results confirm the conclusions we draw above, according to which *FF2* and *FF3* force fields give rise to very similar system configurations, but they both significantly differ from what one gets if *FF1* is employed.

Again, using the most representative configuration for each system, we have compared the overall folding features of the Zn^{+2}–$A\beta_{1-16}$ complex in the different physico-chemical conditions we have considered by computing how many residues are found in a α-helix secondary structure. The calculation is performed using the VMD Ramachandran plot routine [44]. The result of the analysis of the solvated systems (see Fig. 2, Fig. 3 and Fig. 4) is that *FF1* and *FF3* yield a larger number of amino acids in an α-helix configuration than *FF2* that is essentially all β-sheet. These differences point to the fact that also the Zn site geometry in turn influences the long-range arrangement of the peptide.

As largely expected, the conclusion we can draw from the MD simulation results is that what makes *FF1* generally different from and less reliable than the other two force fields[6] is not so much the choice of the bonding parameters of the Zn^{+2} ligands (*FF3* has the same bonding parameters as *FF1*) but rather the unphysical values of partial charges assigned to Zn^{+2} and the nearest atoms surrounding it, at variance with the more realistic assignments provided by *FF2* and *FF3* (see Table 2).

3.2. QM/MM simulations

The power of quantum-mechanical calculations is that bond and charge parameters can be self-consistently computed from *first-principle* and not, as one is forced to do in any classical simulation, more or less ingenuously guessed from experience and/or other MD calculations (based on a careful use of the transferability assumption [45]). Quantum calculations thus allow testing the stability of MD configurations, hence the reliability of classical modeling.

In Table 4 we report for each of the six model systems we have considered the distance from the metal of the atoms lying within the Zn^{+2} coordination sphere from which the ONIOM minimization step is started.

3.2.1. S_1 model

We need to note that, because of the peculiar features of the ONIOM computation, in the case of the $(S_1)^{W}$ solvated model, we estimated to be necessary to have in the highest QM layer also those water molecules that are found to be within the 2.5 Å coordination sphere around Zn. For this reason we have considered two different solvated models. In the first model, $(S_1)^{W}_{2w}$ in the following, out of all the water molecules present in the initial configuration, two are added to the highest QM layer (see above in Methods — QM/MM), while all the other water molecules are simply canceled out. In the second model, $(S_1)^{W}_{all}$ in the following, all the remaining water molecules are taken into account but are included at the lowest MM level.

The very reassuring result of the ONIOM optimization step is that in all the three variants of the S_1 model we have considered (i.e. irrespective of how water is treated) the Zn^{+2} ion ends up to be always tetra-coordinated to the nitrogen atoms of His6, His13, and His14 and the carboxyl oxygen of Glu11 (see Table 5). Water molecules are never involved in the Zn coordination. Indeed, the two oxygen atoms, that entered the Zn^{+2} coordination sphere along the MD trajectory (a water molecule and O(Gly9), see Table 3), are pushed away in the course of the ONIOM minimization. As we already noticed, the unphysical Zn^{+2} coordination mode brought up by the MD simulations of the S_1 model is (we believe) due to the unrealistic partial charge assignments of *FF1*. We report in Table 6 the ESP charges computed by Gaussian 03 at the end of the ONIOM geometrical optimization. As expected, this computation leads to a value of the Zn ion partial charge that is quite smaller than the nominal +2 value employed in *FF1*.[7]

As a last observation we note that the geometries of the Zn^{+2} site of the $(S_1)^{W}_{2w}$ and $(S_1)^{W}_{all}$ models are essentially indistinguishable. Thus in the case of the S_2 model, when water is present, we limited the ONIOM analysis to only the $(S_2)^{W}_{2w}$ system.

3.2.2. S_2 model

The ONIOM geometrical optimization of the $(S_2)^{GP}$ and $(S_2)^{W}_{2}$ models does not bring any substantial modification of the initial Zn^{+2} site structure, leaving the metal in its initial tetra-coordination mode, with the nitrogen atoms of His6, His13, and His14 and the carboxyl oxygen of Glu11 as ligands (see Table 6) and almost unaltered geometry.

3.2.3. S_3 model

Given the strong similarity of the S_2 and S_3 structures one obtains after the steepest descent minimization of the MD classical configurations, it was unnecessary to repeat the ONIOM optimization in this case.

[5] A penta-coordination has been observed in EXAFS experiments on Zn^{+2}–$A\beta_{1-16}$ complexes in solution with the fifth ligand being a water oxygen [10,11]. In this case, however, four of the ligands are histidines, implying that Zn^{+2} (which is present at a sub-stoichiometric concentration) is binding pairs of $A\beta_{1-16}$-peptides.

[6] Except for what *FF1* yields on the number of amino acids in an α-helix configuration that is in a slightly better agreement with experimental results [11] than what one finds with *FF2* and *FF3*.

[7] Since only the charges of the atoms belonging to the Zn^{+2} coordination sphere are reported, their sum may not be exactly equal to zero.

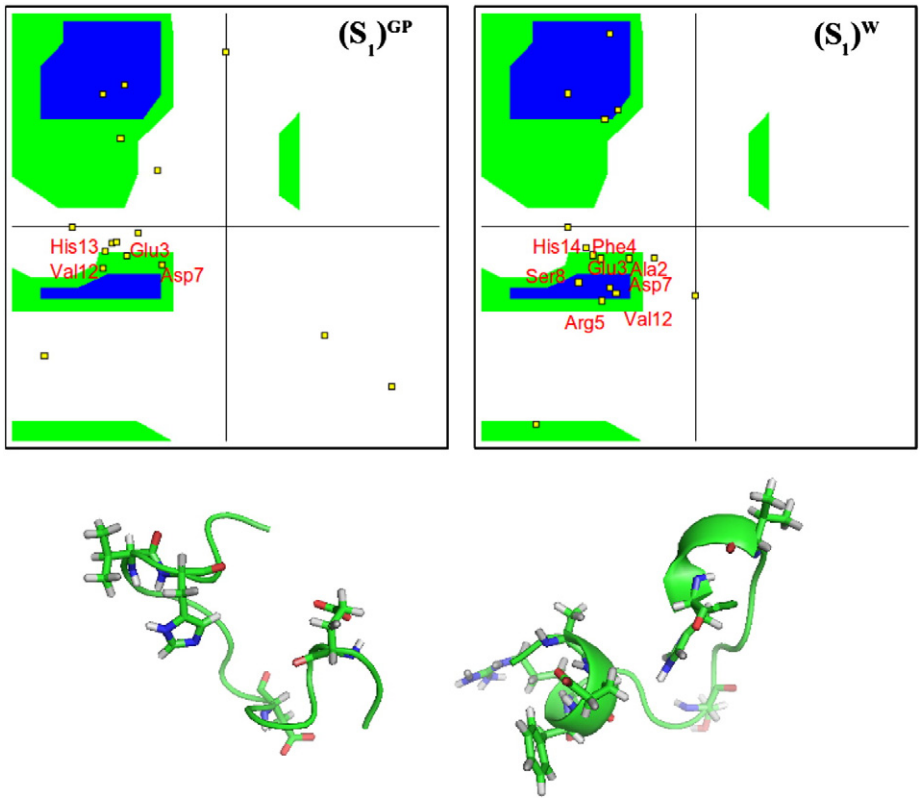

Fig. 2. Upper panel: Ramachandran plots relative to the most representative configurations of the classical MD simulation at 300 K for $(S_1)^{GP}$ and $(S_1)^{W}$ systems (see text, end of Methods section). Lower panel: cartoons of the most representative configurations (residues in α-helix are drawn as sticks).

In summary the main results of the QM/MM calculations are the following. First of all one unequivocally finds that in the Zn^{+2}–$A\beta_{1-16}$ complex the metal ion likes to be locally tetra-coordinated. Secondly all the computed ESP charges are seen not to depend much on the details of the simulated model system, and clearly favor the *FF2*/*FF3* partial charges.

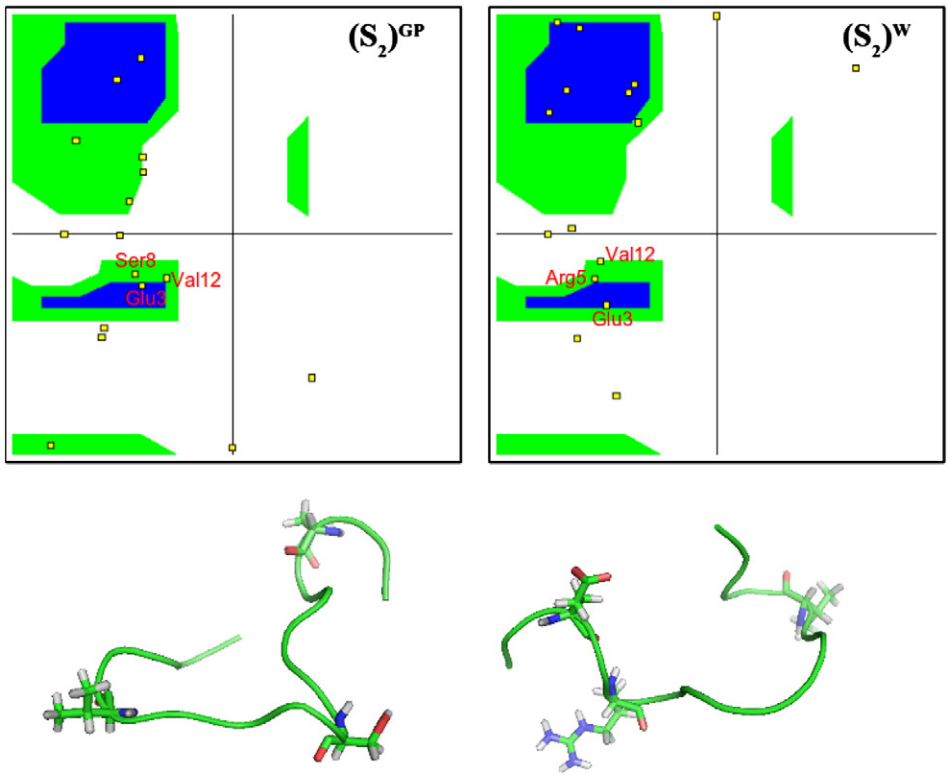

Fig. 3. Same as Fig. 1 for $(S_2)^{GP}$ and $(S_2)^{W}$ systems.

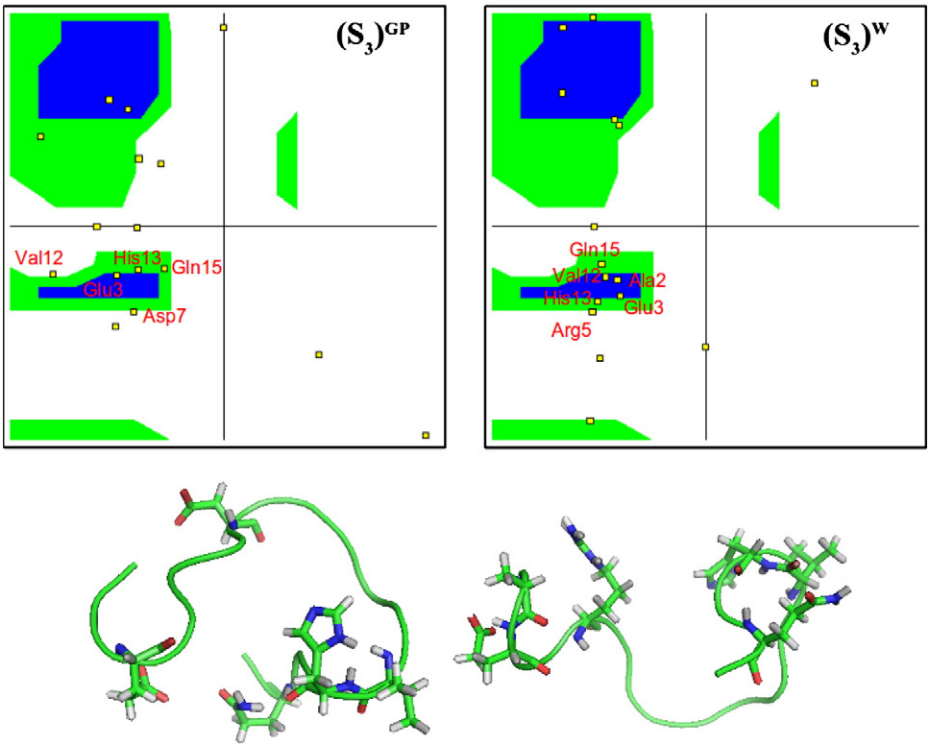

Fig. 4. Same as Fig. 1 for $(S_3)^{GP}$ and $(S_3)^{W}$ systems.

4. Conclusions

In this paper we have presented complementary classical and hybrid QM/MM calculations of the Zn^{+2}–$A\beta_{1-16}$ complex with and without water. We have shown that the micro-environmental properties of the metal site are specially influenced by the partial charges attributed to the metal and the nearest atoms surrounding it, while the presence of the solvent mainly influences the α-helix propensity of the peptide.

For what concerns the Zn^{+2} partial charge, by setting it to its nominal value, i.e. +2, one ends up in classical MD with the metal coordinated to six atoms in a configuration that, however, is not stable under the subsequent QM/MM optimization. The situation changes drastically if the Zn^{+2} partial charge is reduced to something like +0.5. In this case a tetra-coordination geometry, compatible with what is experimentally known [18,25,26,28,31] and stable under QM/MM, is instead found. It should be noted that, on the other hand no appreciable modifications of the Zn^{+2} binding mode is visible if force field bond constants are varied (within reasonable ranges).

The interesting outcome of QM/MM calculations is twofold. First of all we see that the optimized metal coordination geometry is independent of the details of the classical force field used in MD and the way the solvent is treated in QM/MM. This stability is the result of the fact that in the QM/MM computational approach Zn^{+2} is endowed with an effective charge that is self-consistently determined by the quantum-mechanical treatment of the valence electrons of the atoms comprised in the Zn^{+2} binding site. Secondly, one finds that the final long-range arrangement of the peptide secondary structure strongly depends, instead, on whether the peptide is solvated or not.

We regard these conclusions as physically rather satisfactory as they show that the local environment of the Zn^{+2} binding site is quite stable, if partial charges are correctly chosen, while the structural arrangement of the peptide at large also depends on the long-range physico-chemical properties of the environment.

Moreover we find that the presence of water is necessary to obtain the kind of overall peptide folding properties that is visible in FTIR experiments of ref. [11]. Finally, we have identified a good quality and rather simple Zn^{+2} force field, namely *FF3*, that appears to be particularly well adapted to perform extensive classical MD simulations in the especially important case of β-amyloid peptides.

Naturally one can imagine extending to other similar situations the strategy we have successfully employed in the Zn^{+2} case, bringing it to a workable computational tool capable of validating and optimizing classical metal force fields.

Table 4
Same as in Table 3. Now in columns from 2 to 7 the distances from Zn of the atoms in its coordination sphere at the beginning of the QM/MM calculation (namely as they come out in the last configuration after 0.75 ns MD at 300 K and classical minimization) are reported.

Atom	Distance from Zn (Å)					
	$(S_1)^{GP}$	$(S_1)^{W}$	$(S_2)^{GP}$	$(S_2)^{W}$	$(S_3)^{GP}$	$(S_3)^{W}$
Nδ(His6)	2.21	2.28	2.11	2.10	2.07	2.13
Oε(Glu11)	2.16	2.24	2.11	2.13	2.05	2.08
Nε(His13)	2.14	2.21	2.12	2.10	2.06	2.08
Nδ(His14)	2.20	2.34	2.11	2.12	2.07	2.07
O(Gly9)	2.08	2.11				
O(H_2O)		2.20				

Table 5
Detailed geometry of the Zn coordination sphere in the three configurations (see text) of the S_1 model and the two configurations of the S_2 model at the end of the QM/MM calculation. Only four atoms remain within the Zn coordination sphere.

Atom	Distance from Zn (Å)				
	$(S_1)^{GP}$	$(S_1)^{W}{}_{2w}$	$(S_1)^{W}{}_{all}$	$(S_2)^{GP}$	$(S_2)^{W}{}_{2}$
Nδ(His6)	2.10	2.05	2.07	2.07	2.03
Oε(Glu11)	1.98	1.96	1.99	1.93	1.94
Nε(His13)	2.09	2.09	2.14	2.08	2.07
Nδ(His14)	2.13	2.05	2.05	2.09	2.07

Table 6
A comparison of the ESP partial charges of Zn^{2+} and atoms listed in Table 5 computed after the ONIOM minimization with those employed in the *FF1*, *FF2* and *FF3* force fields.

Atom	ESP from ONIOM					Classical force field		
	$(S_1)^{GP}$	$(S_1)^{W}{}_{2w}$	$(S_1)^{W}{}_{all}$	$(S_2)^{GP}$	$(S_2)^{W}{}_{2}$	*FF1*	*FF2*	*FF3*
Zn	0.94	0.82	0.80	0.89	0.70	2	0.5	0.7
Nδ1(His6)	−0.48	−0.25	−0.40	−0.32	−0.22	−0.7	−0.3	−0.11
Oε(Glu11)	−0.62	−0.70	−0.77	−0.62	−0.61	−0.76	−0.76	−0.81
Nε2(His13)	−0.49	−0.37	−0.47	−0.40	−0.30	−0.7	−0.3	0.01
Nδ1(His14)	−0.26	−0.26	−0.16	−0.65	−0.13	−0.7	−0.3	−0.11

Acknowledgments

We wish to thank G.C. Rossi for the discussions and for a careful reading of the manuscript. Partial support from PRIN2008 and INFN TO61-initiative is also acknowledged.

Appendix A. Supplementary data

Supplementary data to this article can be found online at http://dx.doi.org/10.1016/j.bpc.2013.07.002.

References

[1] S.B. Prusiner, Shattuck lecture: neurodegenerative diseases and prions, The New England Journal of Medicine 344 (2001) 1516–1526.
[2] M.B. Pepys, Pathogenesis, diagnosis and treatment of systemic amyloidosis, Philosophical Transactions of the Royal Society of London B 356 (2001) 203–211.
[3] S. Gandy, The role of cerebral amyloid β accumulation in common forms of Alzheimer disease, Journal of Clinical Investigation 115 (2005) 1121–1129.
[4] A.I. Bush, The metallobiology of Alzheimer's disease, Trends in Neurosciences 26 (2003) 207–214.
[5] K.J. Barnham, C.L. Masters, A.I. Bush, Neurodegenerative diseases and oxidative stress, Nature Reviews Drug Discovery 3 (2004) 205–214.
[6] R.D. Therry, The pathogenesis of Alzheimer disease: an alternative to the amyloid hypothesis, Journal of Neuropathology and Experimental Neurology 55 (1996) 1023–1025.
[7] M.A. Lovell, J.D. Robertson, W.J. Teesdale, J.L. Campbell, W.R. Markesbery, Copper, iron and zinc in Alzheimer's disease senile plaques, Journal of Neurological Sciences 158 (1998) 47–52.
[8] C. Opazo, M.I. Barria, F.H. Ruiz, N.C. Inestrosa, Copper reduction by copper binding proteins and its relation to neurodegenerative diseases, Biometals 16 (2003) 91–98.
[9] R.A. Cherny, C.S. Atwood, M.E. Xilinas, D.N. Gray, W.D. Jones, C.A. McLean, K.J. Barnham, I. Volitakis, F.W. Fraser, Y.S. Kim, et al., Treatment with a copper–zinc chelator markedly and rapidly inhibits β-amyloid accumulation in Alzheimer's disease transgenic mice, Neuron 30 (2001) 665–676.
[10] F. Stellato, G. Menestrina, M. Dalla Serra, C. Potrich, R. Tomazzolli, W. Meyer-Klaucke, S. Morante, Metal binding in amyloid β-peptides shows intra- and inter-peptide coordination modes, European Biophysics Journal 35 (2006) 340–351.
[11] V. Minicozzi, F. Stellato, M. Comai, M. Dalla Serra, C. Potrich, W. Meyer-Klaucke, S. Morante, Identifying the minimal copper- and zinc-binding site sequence in amyloid-β peptides, Journal of Biological Chemistry 283 (2008) 10784–10792.
[12] S. Morante, The role of metals in beta-amyloid peptide aggregation: X-ray spectroscopy and numerical simulations, Current Alzheimer Research 5 (2008) 508–524.
[13] M.A. Smith, P.L.R. Harris, L.M. Sayre, G. Perry, Iron accumulation in Alzheimer disease is a source of redox-generated free radicals, Proceedings of the National Academy of Sciences of the United States of America 94 (1997) 9866–9868.
[14] S.C. Drew, C.J. Noble, C.L. Masters, G.R. Hanson, K.J. Barnham, Pleomorphic copper coordination by Alzheimer's disease amyloid-β peptide, JACS 131 (2009) 1195–1207.
[15] C. Sarell, C.D. Syme, S. Rigby, J.H. Viles, Copper(II) binding to amyloid-beta fibrils of Alzheimer's disease reveals a pico-molar affinity; stoichiometry and coordination geometry is independent of a oligomeric form, Biochemistry 48 (2009) 4388–4402.
[16] J. Danielsson, R. Pierattelli, L. Banci, A. Graeslund, High-resolution NMR studies of the zinc-binding site of the Alzheimer's amyloid β-peptide, FEBS Journal 274 (2007) 46–59.
[17] A.K. Tickler, D.G. Smith, G.D. Ciccotosto, D.J. Tew, C.C. Curtain, D. Carrington, C.L. Masters, A.I. Bush, R.A. Cherny, R. Cappai, J.D. Wade, K.J. Barnham, Methylation of the imidazole side chains of the Alzheimer disease amyloid-β peptide results in abolition of superoxide dismutaselike structures and inhibition of neurotoxicity, Journal of Biological Chemistry 280 (2005) 13355–13363.
[18] S. Zirah, S.A. Kozin, A.K. Mazur, A. Blond, M. Cheminant, I. Ségalas-Milazzo, P. Debey, S. Rebuffat, Structural changes of region 1–16 of the Alzheimer disease amyloid β-peptide upon zinc binding and in vitro aging, Journal of Biological Chemistry 281 (2006) 2151–2161.
[19] C.D. Syme, J.H. Viles, Solution ^{1}H NMR investigation of Zn^{2+} and Cd^{2+} binding to amyloid-beta peptide (Aβ) of Alzheimer's disease, BBA 1764 (2006) 246–256.
[20] D.F. Raffa, R. Gomez-Balderas, P. Brunelle, G.A. Rickard, A. Rauk, Ab initio model studies of copper binding to peptides containing a His–His sequence: relevance to the β-amyloid peptide of Alzheimer's disease, Journal of Biological Inorganic Chemistry 10 (2005) 887–902.
[21] D.F. Raffa, G.A. Rickard, A. Rauk, Ab initio modelling of the structure and redox behaviour of copper(I) bound to a His–His model peptide: relevance to the β-amyloid peptide of Alzheimer's disease, Journal of Biological Inorganic Chemistry 12 (2007) 147–164.
[22] A. Rauk, Why is the amyloid beta peptide of Alzheimer's disease neurotoxic? Dalton Transactions (2008) 1273–1282.
[23] D.F. Raffa, A. Rauk, Molecular dynamics study of the beta amyloid peptide of Alzheimer's disease and its divalent copper complexes, The Journal of Physical Chemistry. B 111 (2007) 3789–3799.
[24] Y. Mantri, M. Fioroni, M.H. Baik, Computational study of the binding of CuII to Alzheimer's amyloid-β peptide: Do Aβ42 and Aβ40 bind copper in identical fashion? Journal of Biological Inorganic Chemistry 13 (2008) 1197–1204.
[25] S. Furlan, G. La Penna, Modeling of the Zn^{2+} binding in the 1–16 region of the amyloid β peptide involved in Alzheimer's disease, ChemPhysChem 11 (2009) 6468–6481.
[26] T. Marino, N. Russo, M. Toscano, M. Pavelka, On the metal ion (Zn^{2+}, Cu^{2+}) coordination with beta-amyloid peptide: DFT computational study, Interdiscipl Sci Comput Life Sci 2 (2010) 57–69.
[27] P. Giannozzi, K. Jansen, G. La Penna, V. Minicozzi, S. Morante, G.C. Rossi, F. Stellato, Zn induced structural aggregation patterns of β-amyloid peptides by first-principle simulations and XAS measurements, Metallomics 4 (2012) 156–165.
[28] Y. Miller, B. Ma, R. Nussinov, Zinc ions promote Alzheimer Aβ aggregation via population shift of polymorphic states, Proceedings of the National Academy of Sciences of the United States of America 107 (2010) 9490–9495.
[29] W. Li, J. Zhang, Y. Su, J. Wang, M. Qin, W. Wangl, Effects of zinc binding on the conformational distribution of the amyloid-β peptide based on molecular dynamics simulations, The Journal of Physical Chemistry. B 111 (2007) 13814–13821.
[30] R. Zhou, B.J. Berne, Can a continuum solvent model reproduce the free energy landscape of a β-hairpin in water? Proceedings of the National Academy of Sciences of the United States of America 99 (2002) 12777–12782.
[31] M.B. Peters, Y. Yang, B. Wang, L. Fusti-Molnar, M.N. Weaver, K.M. Jr Merz, Structural survey of zinc-containing proteins and development of the Zinc AMBER Force Field, (ZAFF), Journal of Chemical Theory and Computation 6 (2010) 2935–2947.
[32] M. Eichinger, P. Tavan, J. Hutter, M. Parrinello, A hybrid method for solutes in complex solvents: density functional theory with empirical force fields, Journal of Chemical Physics 110 (1999) 10452–10467.
[33] E. Gaggelli, A. Janicka-Klos, E. Jankowska, H. Kozlowski, C. Migliorini, E. Molteni, D. Valensin, G. Valensin, E. Wieczerzak, NMR studies of the Zn^{2+} interactions with rat and human β-amyloid (1–28) peptides in water–micelle environment, The Journal of Physical Chemistry. B 112 (2008) 100–109.
[34] B. Hess, C. Kutzner, D. van der Spoel, E. Lindahl, GROMACS 4: algorithms for highly efficient, load-balanced, and scalable molecular simulation, Journal of Chemical Theory and Computation 4 (2008) 435–447.
[35] T. Tuccinardi, A. Martinelli, E. Nuti, P. Carelli, F. Balzano, G. Uccello-Barretta, G. Murphy, A. Rossello, Amber force field implementation, molecular modelling study, synthesis and MMP-1/MMP-2 inhibition profile of (R)-and (S)-N-hydroxy-2-(N-isopropoxybiphenyl-4-ylsulfonamido)-3 methylbutanamides, Bioorganic & Medicinal Chemistry 14 (2006) 4260–4276.
[36] L. Banci, P. Carloni, G. La Penna, P.L. Orioli, Molecular dynamics studies on superoxide dismutase and its mutants: the structural and functional role of Arg 143, JACS 114 (1992) 6994–7001.
[37] S. Nosé, A unified formulation of the constant temperature *molecular* dynamics methods, Molecular Physics 52 (1984) 255–268.
[38] T. Darden, D. York, L. Pedersen, Particle Mesh Ewald—an N. Log(N) method for Ewald sums in large systems, Journal of Chemical Physics 98 (1993) 10089–10092.
[39] M. Svensson, S. Humbel, R.D.J. Froese, T. Matsubara, S. Sieber, K. Morokuma, ONIOM: a multilayered integrated MO + MM method for geometry optimizations and single point energy predictions. A test for Diels–Alder reactions and $Pt(P(t\text{-}Bu)_3)_2 + H_2$ oxidative addition, Journal of Physical Chemistry 100 (1996) 19357–19363.
[40] S. Humbel, S. Sieber, K. Morokuma, The IMOMO method: integration of different levels of molecular orbital approximations for geometry optimization of large systems. Test for n-butane conformation and S_N2 reaction: RCl + Cl^-, Journal of Chemical Physics 105 (1996) 1959–1967.
[41] R.D.J. Froese, K. Morokuma, Hybrid method, in: PvR Schleyer (Ed.), Encyclopedia of Computational Chemistry, Wiley, New York, 1988.
[42] M.J. Frisch, G.W. Trucks, H.B. Schlegel, G.E. Scuseria, M.A. Robb, J.R. Cheeseman, J.A. Montgomery Jr., T. Vreven, K.N. Kudin, J.C. Burant, et al., Gaussian 03, Revision C.02, Gaussian, Inc., Wallingford CT, 2004.
[43] A.K. Rappe, C.J. Casewit, K.S. Colwell, W.A. Goddard, W.M. Skiff, UFF, a full periodic table force field for molecular mechanics and molecular dynamics simulations, JACS 114 (1992) 10024–10035.
[44] W. Humphrey, A. Dalke, K. Schulten, VMD: visual molecular dynamics, Journal of Molecular Graphics 14 (1996) 33–38.
[45] F. Sato, S. Hojo, H. Sun, On the transferability of force field parameters with an ab initio force field developed for sulfonamides, Journal of Physical Chemistry A 107 (2003) 248–257.